

A 4 Interaction of X-rays, Neutrons and Electrons with Matter

David P. DiVincenzo

PGI-2

Forschungszentrum Jülich GmbH

Contents

1	The Basics of Scattering Theory	2
2	The Scattering of Electromagnetic Radiation from Atoms	4
3	Atomic Form Factor for X-rays	7
4	X-ray Absorption and Dispersion	9
5	Electron Scattering	12
6	Neutron Scattering	13
7	Magnetic Neutron Scattering	15

1 The Basics of Scattering Theory

Each of the scattering probes that we discuss here, be they particles or waves, permit, according to the tenets of quantum mechanics, a description of either sort. In fact, the wave theory is the best adapted as the unified framework that we will set up here. The incident beam will be treated as monoenergetic and unidirectional – and thus as a plane wave, with incident wave field

$$\Psi_{inc}(\mathbf{r}) = Ae^{i\mathbf{k}\cdot\mathbf{r}} \quad (1)$$

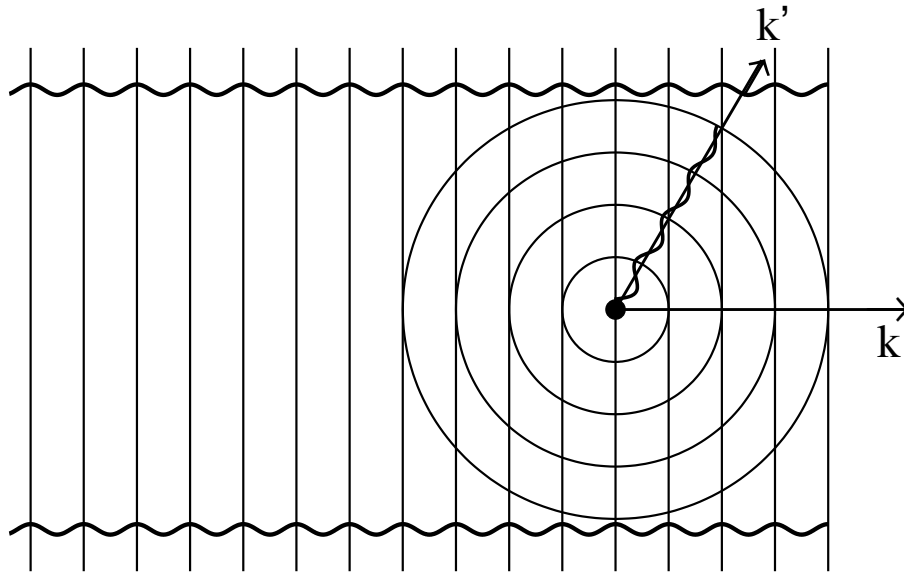


Fig. 1: A schematic of the scattering process from an atomic target. The incident plane wave (wavy line) has wavevector k ; its constant-phase fronts are shown as straight lines. The scattered wave is an outgoing spherical wave (circles) going out in all directions, including in the wavevector direction k' .

The energy of the incident scatterer is a function of the magnitude of the wavevector $|\mathbf{k}|$; for nonrelativistic electrons or neutrons, $E = \hbar^2 k^2 / 2m$, and for light, $E = \hbar ck$. The direction of propagation is of course the direction of the vector \mathbf{k} , which will be conveniently described in spherical polar coordinates using angles $(\theta, \varphi) = \Omega$. We assume that there is a small scattering target fixed at the origin. In the relevant wave equation, this scatterer will be described by a potential energy function $V(\vec{r})$. The “interaction region” $|\mathbf{r}| < r_0$ is assumed to be the only region in which $V(\vec{r}) \neq 0$. Outside this interaction region the wave field also contains an outgoing spherical wave of the form

$$\Psi_{scat} = Af(\Omega) \frac{e^{ikr}}{r} \quad (2)$$

We have specialized to elastic scattering (appropriate for most of the scattering experiments considered in this chapter), so that the magnitude of the incident and scattered wavevectors k are the same.

The quantity $f(\Omega)$ is the central focus of our attention, describing the amount of scattering in the direction of the solid angle Ω . Note that the complex quantity f has units of length – it is a

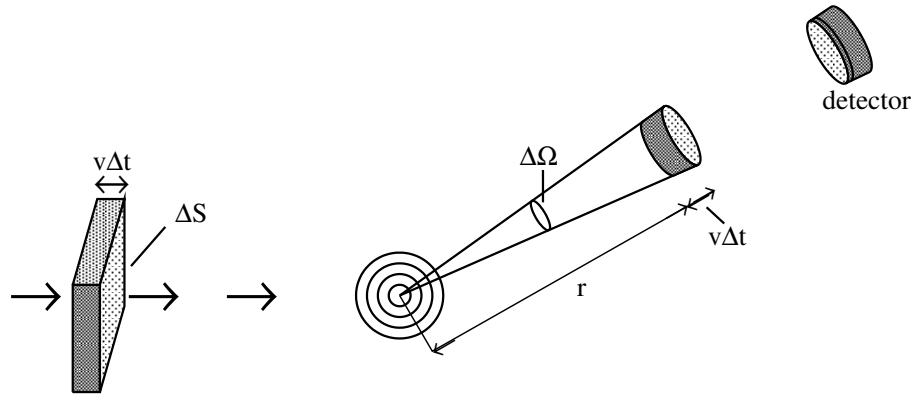


Fig. 2: Geometry of the scattering process.

”scattering length”. It in fact directly indicates the normalized scattering flux $\Delta\sigma(\Omega)$ in a cone of solid angle $\Delta\Omega$ (see Fig. 2), in the direction Ω , for unit incident wave flux density:

$$\Delta\sigma = |f(\Omega)|^2 d\Omega \quad (3)$$

The total scattering cross section is

$$\sigma = \int |f(\Omega)|^2 d\Omega \quad (4)$$

We see that the phase of the complex scattering length $f(\Omega)$ does not appear in any of our expressions; however it is very important in the interference that occurs in scattering from two different scattering centers. This effect is beyond the scope of the present chapter.

For completeness, we note the other important quantity, the differential scattering cross section, which is simply the integrand of the quantity above:

$$\frac{d\sigma}{d\Omega} = |f(\Omega)|^2 \quad (5)$$

We end this section with a simple physical picture of the scattering cross section. Naturally, the above discussion implies that the full wave field is given by the sum of the incident and scattered waves, which is correct in the Born approximation:

$$\Psi_{tot}(\mathbf{r}) = A \left(e^{i\mathbf{k}\cdot\mathbf{r}} + f(\Omega) \frac{e^{ikr}}{r} \right) \quad (6)$$

This Born approximation expression does not take account of the fact that the flux of the incident beam is affected (and depleted) by scattering. The amount by which it is depleted is exactly the flux density through the area σ . One can have a simple picture of this result: the depleting effect of the scatterer is exactly the same as that of a fully absorbing screen with area σ (Figure 2). The common unit for σ in scattering physics is the *barn*, which, at $10^{-28}m^2$, is actually a large unit of area in many areas of particle and nuclear physics. The term originates from the 20th century American taunt to a poor thrower, “You couldn’t hit the broad side of a barn.”

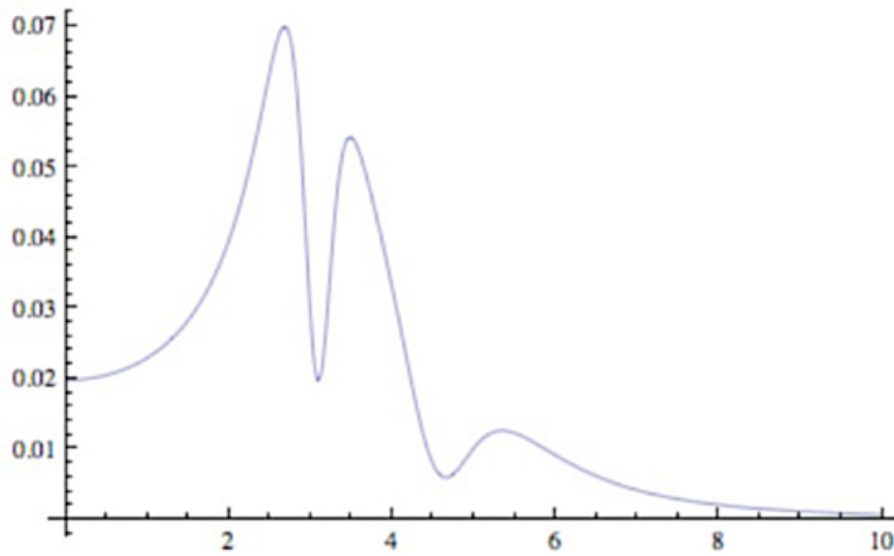


Fig. 3: A schematic of the square of the real part of the polarizability $(\chi'(\omega))^2$ versus frequency ω . We see the low frequency, Rayleigh part (frequency independent), a complex intermediate frequency range in which anomalous dispersion and absorption occur, and then a high-frequency, Thompson part (going like $1/\omega^4$).

2 The Scattering of Electromagnetic Radiation from Atoms

While we will in this school primarily be concerned with high-energy scattering probes such as X-rays, we begin this discussion at the low-energy (that is, the low-frequency) end of the spectrum. An electromagnetic wave comprises transverse, perpendicular oscillating electric and magnetic fields. We first consider the effect of the electric fields on a target atom. At low frequencies, below that of any atomic resonances, the applied field will polarize the electrons bound to the atom, producing an electric polarization P proportional to the strength of the electric field:

$$P(\omega) = \chi(\omega)E(\omega) \quad (7)$$

At low frequencies, the electric polarizability of the atom $\chi(\omega)$ is independent of frequency ω . The resulting electric dipole oscillating with angular frequency ω , $P(\omega)e^{i\omega t}$, will radiate an outgoing spherical wave – this is the scattered wave of our general scattering theory. From classical electromagnetic theory, the efficiency with which this dipole radiates energy scales like the fourth power of the frequency; the net result for the scattering cross section is the formula for *Rayleigh scattering*:

$$\sigma_R(\omega) = \frac{8\pi}{3} \frac{\omega^4}{(4\pi\epsilon_0 c^2)^2} (\chi(0))^2 \quad (8)$$

Recall that this ω^4 dependence gives Rayleigh's explanation that the sky is blue.

Passing over the visible and ultraviolet region of the spectrum where atoms show complex resonant behavior in their scattering cross section (Figure 3), we consider a regime where the frequency is high enough that the binding of the electron to the atom is *irrelevant*; the electron oscillates as if it were in free space. In this regime a calculation of the oscillating dipole $P(\omega)$ is again straightforward, since it simply requires the calculation of the periodic displacement of a free particle subject to a sinusoidal force. The result in this regime is

$$\chi(\omega) = \frac{e^2}{m_e \omega^2} \quad (9)$$

The higher the frequency, the smaller the polarizability, because the electron has a shorter time in which to move. The scattering formula Eq. (8) still applies, so we get the simple, frequency-independent result for the cross section contribution per electron:

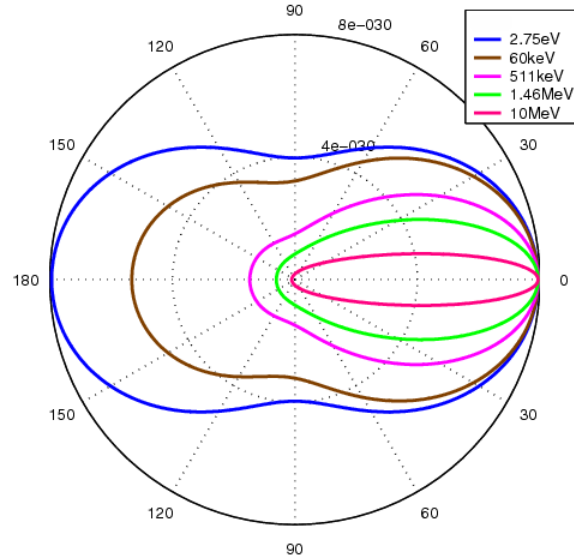


Fig. 4: Polar plot of the Klein-Nishina formula for the differential scattering cross section of X-rays by electrons. At low frequency the scattering goes to that of a classical dipole; at high frequency (the Compton regime) the cross section becomes more and more forward directed, best described as energy- and momentum-conserving photon-electron collisions. From [1].

$$\sigma_T = \frac{8\pi}{3} r_e^2 \quad (10)$$

This is the regime of *Thompson scattering*. Here

$$r_e = \frac{1}{4\pi\epsilon_0} \frac{e^2}{m_e c^2} \approx 2.8 \times 10^{-13} \text{ cm} \quad (11)$$

is the so-called *classical electron radius*.

Even though the binding of the electron to the atomic nucleus is irrelevant in the Thompson scattering regime, it should be understood that, in the regime of low excitation intensity, the nevertheless remains associated with the atom, so long as the distance over which the electron travels under the influence of the time-oscillatory force is much smaller than the atomic radius. In this regime, X-ray scattering is non-destructive. Naturally, if the excitation intensity is raised to the point where this oscillation distance becomes comparable to or greater than the atomic

radius, we enter the regime of *high-intensity effects*, which can very realistically be achieved with strong X-ray sources such as the free-electron laser (FEL). In that case the X-ray probe is destructive, causing ionization and disruption of chemical structure, so the time available for this scattering probe to give useful information about condensed matter is limited.

Of course a more complete calculation is possible; the result for the differential cross section is

$$\frac{d\sigma}{d\Omega} = \frac{r_e^2}{2} (1 + \cos^2 \theta) . \quad (12)$$

The angular dependence appears in Fig. 3, showing the dipolar form that is also characteristic of the Rayleigh scattering regime. This figure shows the result of a much more general calculation due to Klein and Nishina [1], who calculated this scattering taking quantum and relativistic effects into account. The *Klein-Nishina formula* for the differential cross section is

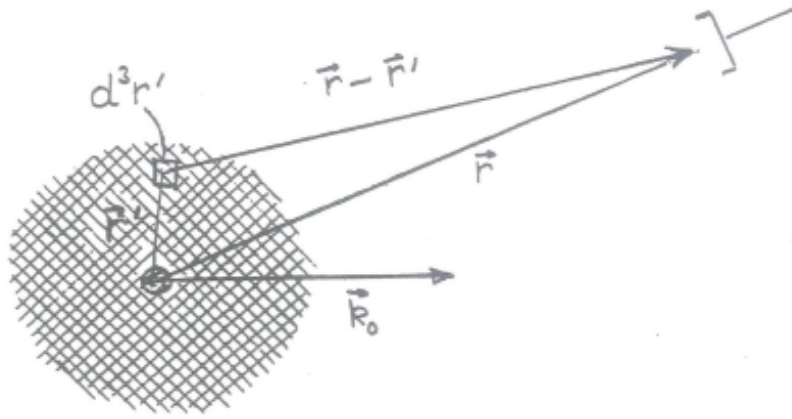


Fig. 5: Scattering geometry for discussion of atomic form factor.

$$\frac{d\sigma}{d\Omega} = \frac{r_e^2}{2} P(\omega, \theta)^2 (P(\omega, \theta) + P(\omega, \theta)^{-1} - 1 + \cos^2 \theta) . \quad (13)$$

Here the factor

$$P(\omega, \theta) = \frac{1}{1 + (\hbar\omega/m_e c^2)(1 - \cos \theta)} \quad (14)$$

has a simple kinematical interpretation when we take the quantum point of view and consider the light to consist of particles (photons): it is the ratio of the photon energy after the scattering event to its original energy before scattering. Note that in the limit of small ω , $P(\omega, \theta) = 1$ and this expression reduces to the one for Thompson scattering. At high frequencies, when the photon energy $\hbar\omega$ becomes comparable to the rest energy of the electron $m_e c^2 = 511\text{keV}$, the scattering takes on a different character, and we enter the regime of *Compton scattering*. The scattering cross section becomes much more forward-directed, as we can see from the figure; the energetic photon suffers less and less of a deflection during the scattering from the electron, the higher its energy is.

3 Atomic Form Factor for X-rays

The Thompson scattering formula is clearly not the whole story of X-ray scattering from an atom. Even in the (considerable) frequency range in which The scenario for Thompson scattering applies (scattering from quasi-free electrons), we need to take account of the fact that the scattering is from the cloud of electrons that is bound to the atom. This means, in short, that the scatterers are not all at the origin of the coordinate system, and we must do a calculation to sum up their contributions.

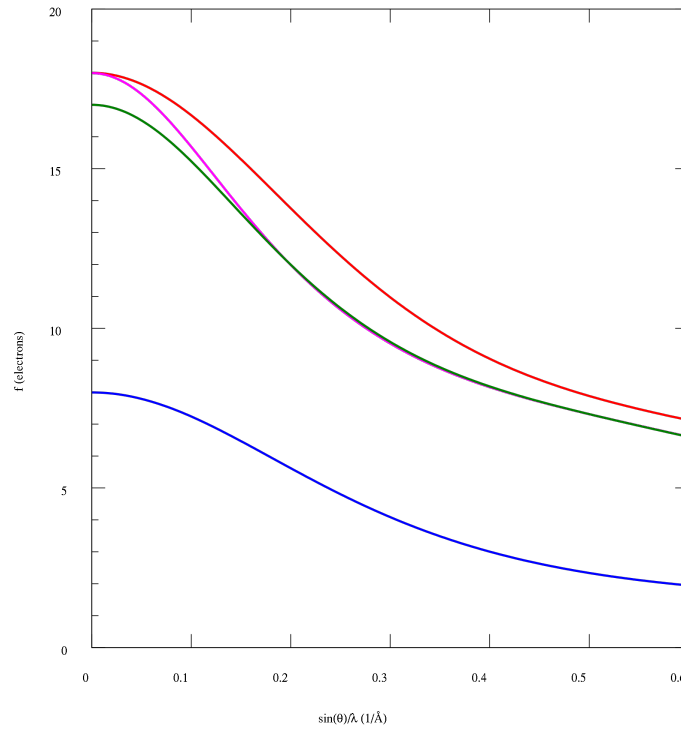


Fig. 6: The atomic form factor $f(Q)$ for several ions and elements, versus $\sin(\theta)/\lambda$. λ is wavelength, θ is scattering angle; with another 4π factor this expression is the scattering wavevector Q . Note that $f(0) = Z$ Z = total number of electrons, not nuclear charge). From top to bottom these curves are for K^+ , Cl^- (note that these have the same number of electrons), Cl and O . From [2].

Referring to the figure, we consider each volume element d^3r' to be a source of Thompson scattering with a strength governed by the probability that an electron is found in this volume element, which is given by the electron density function according to $n(\mathbf{r}')d^3r'$. The spherical wave that is emitted from that element involves the factor

$$n(\mathbf{r}')d^3r' \frac{e^{ik_0|\mathbf{r}-\mathbf{r}'|}}{|\mathbf{r}-\mathbf{r}'|} e^{i\mathbf{k}_0 \cdot \mathbf{r}'} \quad (15)$$

Note that the final factor comes from the phase of the incident plane wave at the scattering point \mathbf{r}' . The overall scattering strength is given by integrating this quantity over the electron cloud:

$$\int d^3r' n(\mathbf{r}') \frac{e^{ik_0|\mathbf{r}-\mathbf{r}'|}}{|\mathbf{r}-\mathbf{r}'|} e^{i\mathbf{k}_0 \cdot \mathbf{r}'} \quad (16)$$

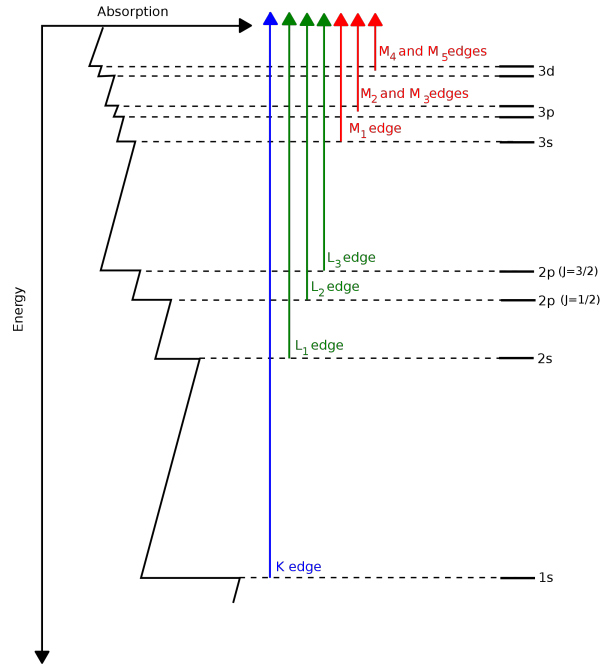


Fig. 7: Schematic of X-ray absorption structure, including many edges, for a typical atom with many inner shells. From [3].

Note that the angular factor from, e.g., the Thompson differential cross section formula will not appear inside this integral, since we will consider only the far field (i.e., $|\mathbf{r}| \gg |\mathbf{r}'|$), so that the angular dependence can be put on as an overall factor once the integral is done.

Since $|\mathbf{r} - \mathbf{r}'| = r - \hat{\mathbf{r}} \cdot \mathbf{r}'$, we can approximate the integrand by

$$\frac{e^{ik_0|\mathbf{r}-\mathbf{r}'|}}{|\mathbf{r} - \mathbf{r}'|} e^{i\mathbf{k}_0 \cdot \mathbf{r}'} \approx \frac{1}{r} e^{ik_0 r} e^{i(\mathbf{k}_0 - \mathbf{k}_1) \cdot \mathbf{r}'} \quad (17)$$

Here $\mathbf{k}_1 = \hat{\mathbf{r}} k_0$. We see here appearing the *scattering wavevector*

$$\mathbf{Q} = \mathbf{k}_0 - \mathbf{k}_1 \quad (18)$$

With this we write our scattering amplitude

$$\int d^3 r' n(\mathbf{r}') e^{i\mathbf{Q} \cdot \mathbf{r}'} \frac{e^{ik_0 r}}{r} = f_a(\mathbf{Q}) \frac{e^{ik_0 r}}{r} \quad (19)$$

We identify the Fourier transform of the atomic electron density,

$$f_a(\mathbf{Q}) = \int d^3 r' n(\mathbf{r}') e^{i\mathbf{Q} \cdot \mathbf{r}'} \quad (20)$$

as the *atomic form factor* for X-ray scattering. It is a factor that must be accounted for in other applications of the scattering theory (e.g., for Bragg scattering). For example, it appears this way in the Thompson scattering differential cross section for an atom,

$$\frac{d\sigma}{d\Omega} = \frac{r_e^2}{2} |f_a(\mathbf{Q})|^2 (1 + \cos^2 \theta) \quad (21)$$

We can see several features of the atomic form factor from Fig. 6. It is of course isotropic for atoms, so this it depends only on $|\mathbf{Q}|$. Its value at zero is very simple:

$$f_a(0) = Z \quad (22)$$

Z being the total electron number of the atom or ion. The figure shows two cases for which this number is the same, namely for the ions K^+ and Cl^- . The extension of these functions is the reciprocal of the extent of the atomic electron cloud in real space; thus we can observe that the Cl^- ion is considerably more extended than K^+ .

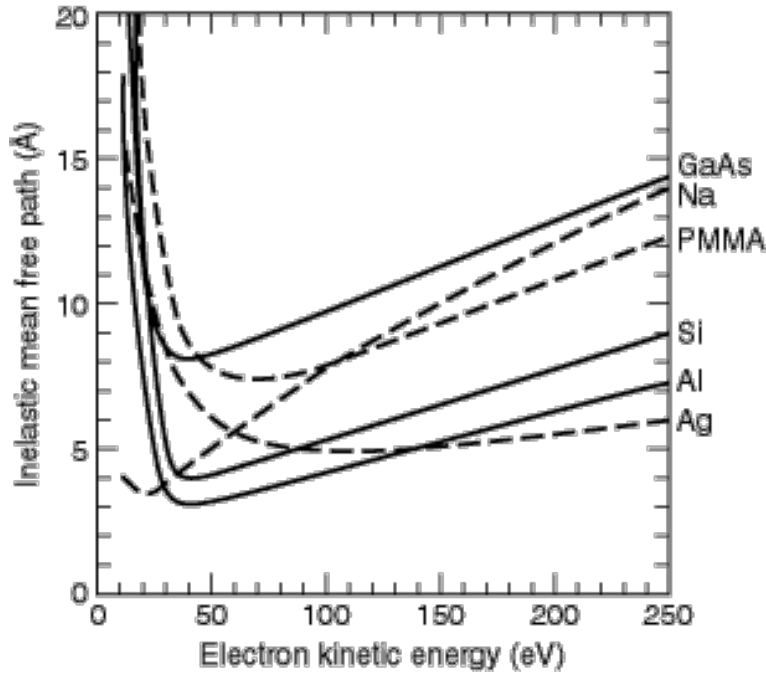


Fig. 8: Electron inelastic mean free path versus incident electron energy, for a range of materials. After [4].

4 X-ray Absorption and Dispersion

Our discussion above has so far ignored the phenomenon of absorption of radiation. We can trace this to our implicit assumption in Eq. (7) that the polarization vector is in-phase with the applied electric field, so that the polarizability function $\chi(\omega)$ is real. In fact the polarization has an out of phase component as well; elementary electromagnetic theory shows that a polarization oscillating out of phase with the electric field results in absorption of energy. Thus, we write the polarizability function as the sum of the real and an imaginary part:

$$\chi(\omega) = \chi'(\omega) + i\chi''(\omega) \quad (23)$$

For atoms, $\chi''(\omega)$ in the X-ray regime is fairly featureless, except for sharp *X-ray edges* that appear when the radiation can eject electrons from the inner electronic shells of the atom. Figure 7 shows the occurrence of these edges, and how they are interpreted in the shell model.

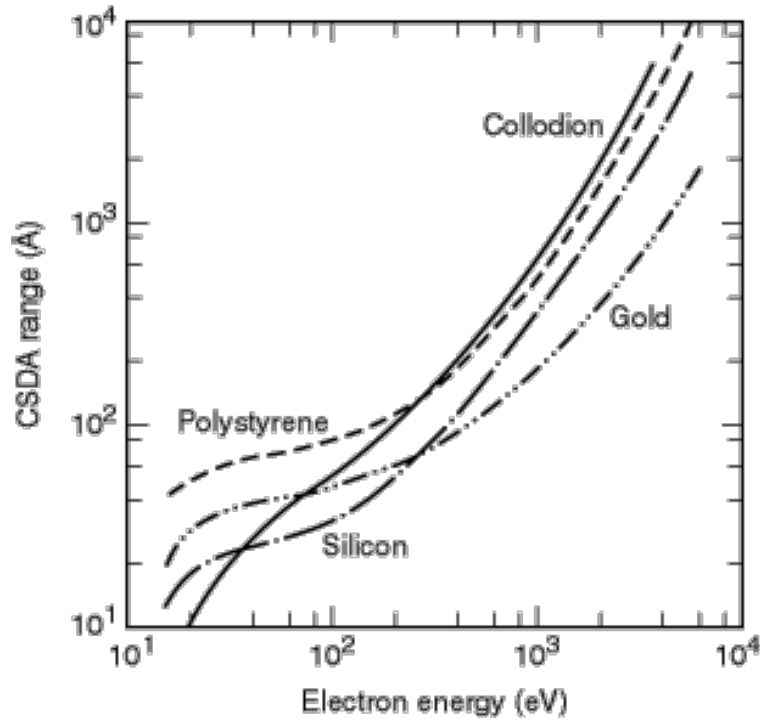


Fig. 9: Continuous Stopping Distance Approximation (CSDA) range of electrons vs. electron energy. After [4].

The occurrence of *dispersion*, significant variation in the lossless response $\chi'(\omega)$, is intimately tied to the appearance of structure in the lossy $\chi''(\omega)$ as exemplified by edges. This connection is embodied in the *Kramers-Kronig relations*. These relations for the $\chi'(\omega)$ function are

$$\chi'(\omega) = \frac{1}{\pi} PV \int_{-\infty}^{\infty} \frac{\chi''(\omega')}{\omega' - \omega} d\omega', \quad (24)$$

$$\chi''(\omega) = -\frac{1}{\pi} PV \int_{-\infty}^{\infty} \frac{\chi'(\omega')}{\omega' - \omega} d\omega'. \quad (25)$$

The derivation of these relations is usually presented as an exercise involving Cauchy's theorem from complex analysis. I will take a moment to review a less rigorous but more physically informative demonstration involving only the elementary features of the Fourier transform. This derivation makes it more clear that the one and only one premise on which the Kramers-Kronig relations are based is the *causality* of the response of the system during scattering. Imagine that the scattering wave impinges as a wave packet on the scatterer, so that the time dependent electric field $E(t)$ becomes non-zero only after $t = 0$. The temporal polarization response is given using the Fourier transform of the polarizability function:

$$P(t) = \int_{-\infty}^{\infty} \chi(t - t') E(t') dt' \quad (26)$$

But because such a physical response is causal, $P(t) = 0$ if $t < 0$; the response cannot begin before the excitation has arrived. But for χ , this implies that

$$\chi(t) = 0 \text{ for } t < 0. \quad (27)$$

Now, we write $\chi(t) = \chi_e(t) + \chi_o(t)$, that is, we decompose χ into a sum of an even function of time and an odd function of time. Because of the causality condition these two functions are related:

$$\chi_e(t) = \text{sgn}(t)\chi_o(t) \quad (28)$$

Here the “sign function” $\text{sgn}(t)$ is $+1$ for $t \geq 0$ and -1 for $t < 0$. Fourier transforming this equation immediately gives the first Kramers-Kronig relation: The Fourier transform of χ_e is purely real and is in fact the real part of $\chi(\omega)$, $\chi'(\omega)$. The Fourier transform of the product is a convolution, the Fourier transform of $\chi_o(t)$ is $i\chi''(\omega)$, and the transform of $\text{sgn}(t)$ is $-i/(\pi\omega)$. The other relation is obtained similarly.

Hopefully this little discussion takes some of the mystery out of these relations. What do they have to do with X-ray scattering? We can see the connection by looking at the model of H. A. Lorentz for absorption based on a model of a damped resonator with resonant frequency ω_0 . This is a good model for an electron bound in an atom; it captures only qualitatively the X-ray absorption edges, which involve not just the oscillation of the electron but also the ejection of the electrons into a continuum. But the “Lorentzian lineshape” for the absorption in Lorentz’s model is very simple:

$$\chi''(\omega) = \frac{e^2}{m_e} \frac{\Gamma\omega}{(\omega_0^2 - \omega^2)^2 + \Gamma^2\omega^2} \quad (29)$$

Here Γ is a linewidth or damping parameter. The Kramers-Kronig relation above requires that this absorption function be accompanied by the following frequency-dependent in-phase polarizability:

$$\chi'(\omega) = \frac{e^2}{m_e} \frac{\omega_0^2 - \omega^2}{(\omega_0^2 - \omega^2)^2 + \Gamma^2\omega^2}. \quad (30)$$

Note that this expression interpolates between the two low-absorption regimes that we have discussed above: Rayleigh scattering (for $\omega \ll \omega_0$, and Thompson scattering for $\omega \gg \omega_0$). The Kramers-Kronig constraints say that there *must* be a regime of high loss in between, and that the in-phase polarizability much also rise to a much higher value than in either of the two limits (in fact, $\chi'(\omega)_{\text{max}} = e^2/m(2\Gamma\omega_0 + \Gamma^2) \approx e^2/(2m\Gamma\omega_0)$ for $\Gamma \ll \omega_0$). This strong enhancement near an absorption feature of the real part of the polarizability, and therefore of the scattering cross section, and its strong frequency dependence, is known as *anomalous dispersion*. As you will learn elsewhere in this course, this phenomenon is used to enhance the contrast of one atomic element relative to another in X-ray scattering.

I conclude this section with a brief discussion of *magnetic X-ray scattering*. I have so far described the X-ray scattering process as involving only the electric field of the incident wave. Naturally, the electromagnetic wave also has a magnetic component, normal to the direction of propagation and also normal to the electric field. This magnetic field also induces a response, and causes an additional contribution to the scattered spherical wave. Most importantly, this scattering is sensitive to the magnetic state of the target – the scattering from an atom will be different when its spin is up or down. Thus, such contributions to the scattering can distinguish the magnetic state (ferromagnetic, antiferromagnetic, etc.) of a material. Generally, this magnetic contribution to the scattering is weak; the scattering amplitude has a prefactor $\hbar\omega/m_e c^2$, so that this scattering is generically suppressed for X-ray photon energies below 511 keV. Wise use of magnetically-dependent anomalous dispersion can enhance the magnetic signal.

5 Electron Scattering

The basic physics of the scattering of electrons from matter is the same as that for X-ray photons: in the quantum theory the electrons have a wave description, and the basic scenario of scattering, in which there is an incident wave on the target, and an outgoing scattered spherical wave. The important qualitative distinction between electron scattering and X-ray scattering is that the strength of electron scattering is much greater than that of X-rays. Electrons will not penetrate a large thickness of material as X-rays will.

In fact, the scattering cross section for electrons can be deduced directly from the cross section for electromagnetic waves, already discussed above. In the electron wave equation (the Schroedinger equation), the scattering intensity from point \mathbf{r} is determined by the potential function at that point $V(\mathbf{r})$. From a calculation of the scattering problem using this equation, the scattering form factor is given by the expression

$$f^e(Q) = \frac{2m_e e}{\hbar^2} \int_0^\infty \frac{V(r) \sin(qr) r^2 dr}{qr} \quad (31)$$

Note that by convention the form factor for electron scattering also contains the scattering length; this means that it has units of meters, rather than being dimensionless as the X-ray form factor is taken to be.

One further step permits f^e to be related directly to the X-ray form factor, since we can relate the scattering potential $V(\mathbf{r})$ to the electron density $n(r)$ whose fourier transform determines the $f(Q)$ for X-rays. This relation is via the Poisson equation, $\nabla^2 V(\mathbf{r}) = -\frac{e}{\epsilon_0} n(\mathbf{r})$. Fourier transforming this equation and substituting into Eq. (31) gives the *Mott-Bethe formula* for the electron form factor for an atom with atomic number Z :

$$f^e(Q, Z) = \frac{m_e e^2}{2\pi \hbar^2 \epsilon_0} \left(\frac{Z - f(Q, Z)}{Q^2} \right) \quad (32)$$

This equation also includes the form factor Z/Q^2 for the atomic nucleus.

The principal item of practical interest that I will cover here is the theory of the stopping range of low-energy electrons in solid matter. For electrons with an incident energy in the range of 5 keV, the basic picture is that electrons slow down by a large sequence of scatterings in the material, each of which leads to a small loss of energy. We speak of the *continuous slowing down approximation* (CSDA) in calculating the electron range. This calculation again involves the polarizability of constituents $\chi(\omega)$. When summed over a large number of constituents, this response is called the *dielectric function* $\epsilon(Q, \omega)$; this expression singles out polarization leading to a scattering wavevector \mathbf{Q} . Then for an electron traveling with energy E , the probability of energy loss ω over a unit of distance is given by the expression

$$p(E, \omega) = \frac{m_e e^2}{\pi \hbar^2 E} \int_{q_-}^{q_+} \text{Im} \left(\frac{-1}{\epsilon(Q, \omega)} \right) \frac{dQ}{Q} \quad (33)$$

Here $\hbar q_{\pm} = \sqrt{2mE} \pm \sqrt{2m(E - \hbar\omega)}$. $p(E, \omega)$ is known as the differential inverse mean free path. The stopping power $S(E)$, which is the energy loss per unit distance travelled along the electron path, is given by

$$S(E) = \int dE \hbar \omega p(E, \hbar \omega) \quad (34)$$

Finally, the distance over which the electron is stopped (actually, brought to a nominal kinetic energy of 10eV) is the CSDA range $R_0(E)$, given by

$$R_0(E) = \int_{10\text{eV}}^E \frac{dE'}{S(E')} \quad (35)$$

In Fig. 8 we show the inelastic mean free path for electrons in a wide variety of solid materials, over the range of incident energies from 10 eV to 250 eV. This quantity continues to grow almost linearly above this energy, up to 2keV. There are two important things to note about this quantity: it has a minimum at a few tens of eV. Electrons are more penetrating at energies both above and below this. Second, the scale of this mean free path is very small, being a fraction of a nanometer over much of this energy range. Just a couple of atomic layers are effective at blocking the passage of a large fraction of electrons in this energy range.

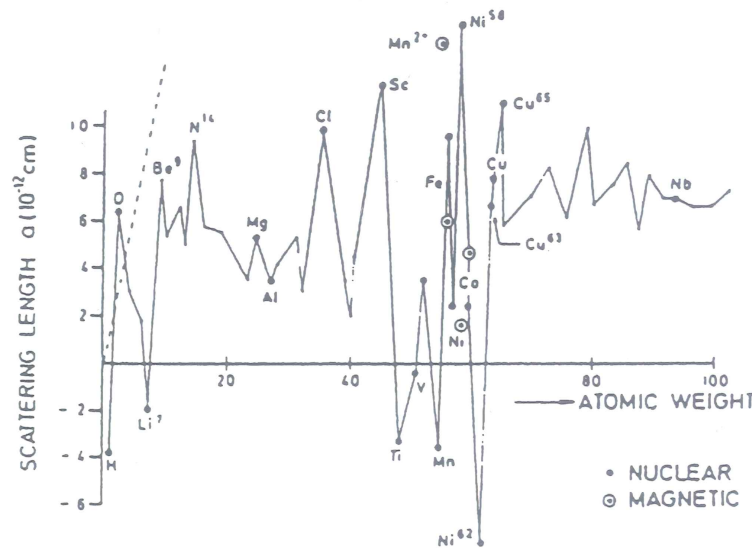


Fig. 10: Scattering length b for the atomic elements, showing the non-monotone dependence of b on atomic weight, even for isotopes of the same element. See [5].

Finally, Fig. 9 shows a sampling of the total travel range for incident electrons (note the much greater range of energies than in the previous figure) for several types of solid materials. Note that the total penetration range never exceeds 1 micrometer for any of the cases shown.

6 Neutron Scattering

The neutron, a particle with no charge, a mass very close to that of the proton, and a spin magnetic moment about 1000 times smaller than that of the electron, is a very useful scattering probe. Neutron beams of high intensity and sharply defined energy and direction can be produced and directed at targets; the neutron's lack of charge permits low-energy neutrons to penetrate deeply into matter. The free neutron is unstable; while its decay is fast compared with many radio-nuclei, at about 10 minutes this time is very long compared with that of the scattering process and detection, so that this decay can be ignored in discussions of neutron scattering.

The energy range of the scattering neutrons is usually “thermal”, meaning that the kinetic energy of the neutrons is reduced by moderation (passage through a non-absorbing material) into the range of $k_B T$ with $T \approx 300\text{K}$. (Moderation to lower energies is possible.) Monochromators pick off well defined energies from this moderated collection of neutrons.

Lacking an electric charge, the neutron still has two means of interacting significantly with matter: first, its magnetic moment makes it sensitive to the magnetic scatterers in the target. Second, the strong nuclear force causes there to be a significant scattering cross section from each magnetic nucleus. It turns out that these contributions are roughly of the same order of magnitude, both are very important in the application of neutron scattering.

We will deal first with the scattering arising from the nuclear force. The strong interaction of the neutron with a many-nucleon atomic nucleus is very complex. However, the description we need of scattering is very much simpler, because at thermal energies, the wavelength of the quantum-mechanical (de Broglie) neutron wave is in the vicinity of 0.1 nm, comparable, in fact, to the internuclear spacings in molecules or solids. This wavelength is very long compared with the range of the strong nuclear force (about 10^{-6} nm). Thus, the neutron-nucleus interaction may be accurately represented as a delta-function at the origin; this is called the Fermi pseudopotential. Fermi writes

$$V(\mathbf{r}) = \frac{2\pi\hbar^2}{m_N} b\delta(\mathbf{r}) \quad (36)$$

Here m_N is the neutron mass. b has dimensions of a length, and is in fact the s-wave scattering length; it is also equal to the neutron form factor, since the delta-function form of the potential means that the form factor has no dependence on the scattering wavevector \mathbf{Q} .

In the simplest view b is just a simple scalar number. We must be a little bit more sophisticated, for several reasons. First, if the target nucleus possesses a non-zero nuclear spin quantum number I , then the scattering depends on the relative angles of the neutron spin vector \mathbf{s} and the nucleus angular momentum vector \mathbf{I} ; in general this spin dependence is quite strong. This effect is included by writing b as

$$b = b_c + \frac{2b_i}{\sqrt{I(I+1)}} \mathbf{s} \cdot \mathbf{I} \quad (37)$$

Thus, the scattering process takes two parameters to describe; for historical reasons, these parameters are called the *coherent* cross section b_c and the *incoherent* cross section b_i . In fact both parameters describe perfectly coherent wave scattering phenomena. However, it is typical in scattering experiments to have no control over the spin state of the target nucleus (there are now many exceptions to this); thus it has been traditional to consider the nuclear spin state to be random, causing the resulting scattering to be incoherent. We will state shortly the consequences of this for scattering from atomic crystals.

The second fact about b that we wish to note is that it also possesses an imaginary part ib'' . As with χ'' above, this constant describes the absorption of neutrons, due to nuclear reactions, during the scattering. Finally, the b “constants” can also be functions of energy. Generally b'' has a linear energy dependence, so that in tabulations the scattering energy must be stated. The real part is in most cases energy independent at thermal energies, although it should be noted that for a small minority of the atomic nuclei, there are already resonances, with anomalous dispersion and enhanced absorption, already at low energies.

All these parameters are accurately measured and can be found tabulated, typically with a couple of digits of accuracy but sometimes much more, for all the isotopes of the periodic table of elements. Unlike the X-ray and electron scattering lengths, which increase monotonically as

one moves down the periodic table, the b parameters, which depend on complex details of nuclear physics, are already large for the lightest nuclei, and vary tremendously from one element to the next, and vary to the same degree even for isotopes of the same element. We show this variation in Fig. 10. So, a crystal of pure He has a perfect periodic structure as seen either by X-ray scattering or neutron scattering (producing “Bragg peaks”, see Chap B1), because pure helium consists almost entirely of one spinless isotope, He-4. But a crystal of pure selenium with equal amounts of Se-74 and Se-76 (these are both natural isotopes of Se, but these are not the natural abundances) looks highly disordered from the point of view of neutron scattering, producing a large component of non-Bragg diffuse scattering, because b_e for Se-74 and Se-76 are very different (0.8 and 12.2 barns, resp.). On the other hand, a pure crystal of arsenic looks disordered for the other reason; while there is only one stable isotope As-75, the four different permitted spin states of the $I=3/2$ As-75 nucleus scatter with considerably different strengths (because $b_i = -0.7$ barns).

7 Magnetic Neutron Scattering

The neutron is a chargeless particle, but it has a magnetic moment, which is about the same in magnitude as the protons, and about 100 times smaller than that of the electron. We analyse the scattering of the neutron from the field arising from the spin of an electron at position \mathbf{r}' :

$$\mathbf{B}_S = \frac{\mu_0}{4\pi} \nabla_{\mathbf{r}} \times \left(\boldsymbol{\mu}_e \times \nabla_{\mathbf{r}} \frac{1}{|\mathbf{r} - \mathbf{r}'|} \right), \quad (38)$$

here $\boldsymbol{\mu}_e = g_e \mu_B \mathbf{s}_e$ is the electron spin magnetic moment; the Bohr magneton is μ_B and the electron spin operator is \mathbf{s}_e . The field arising from electron orbital motion is

$$\mathbf{B}_L = -\frac{\mu_0 e}{4\pi} \frac{\mathbf{v}_e \times (\mathbf{r} - \mathbf{r}')}{|\mathbf{r} - \mathbf{r}'|^3} \quad (39)$$

(we use the Biot-Savart law for a particle with charge $-e$ and velocity \mathbf{v}_e). Here we further consider only the spin field, yielding the potential

$$V(\mathbf{r}) = -\boldsymbol{\mu}_n \mathbf{B}_S = -\boldsymbol{\mu}_n \frac{\mu_0 g_e \mu_B}{4\pi} \nabla_{\mathbf{r}} \times \int d\mathbf{r}' \mathbf{s}_e(\mathbf{r}') \times \nabla_{\mathbf{r}} \frac{1}{|\mathbf{r} - \mathbf{r}'|}, \quad (40)$$

$\boldsymbol{\mu}_n$ is the neutron magnetic moment, and $\mathbf{s}_e(\mathbf{r}')$ is the electronic spin density. The scattering amplitude requires a calculation of a double integral

$$I = \int d\mathbf{r} e^{-i\mathbf{Q}\mathbf{r}} \nabla_{\mathbf{r}} \times \int d\mathbf{r}' \mathbf{s}_e(\mathbf{r}') \times \nabla_{\mathbf{r}} \frac{1}{|\mathbf{r} - \mathbf{r}'|} \quad (41)$$

We perform this evaluation in the Furier domain

$$\frac{1}{r} = \frac{1}{2\pi^2} \int d\mathbf{q} \frac{e^{i\mathbf{q}\mathbf{r}}}{q^2}.$$

One obtains

$$\begin{aligned} I &= -\frac{1}{2\pi^2} \int d\mathbf{r}' \int d\mathbf{r} e^{-i\mathbf{Q}\mathbf{r}} \int d\mathbf{q} \hat{\mathbf{q}} \times \mathbf{s}_e(\mathbf{r}') \times \hat{\mathbf{q}} e^{i\mathbf{q}(\mathbf{r}-\mathbf{r}')} \\ &= -4\pi \hat{\mathbf{Q}} \times \int d\mathbf{r}' \mathbf{s}_e(\mathbf{r}') \times \hat{\mathbf{Q}} e^{-i\mathbf{Q}\mathbf{r}'} \end{aligned} \quad (42)$$

Note that the application of $\nabla_{\mathbf{r}}$ to the exponential term $e^{i\mathbf{q}(\mathbf{r}-\mathbf{r}')}$ results in the simple factors $i\mathbf{q} = iq\hat{\mathbf{q}}$. The integration over \mathbf{r} gives the delta function $\delta(\mathbf{Q} - \mathbf{q})$, permitting the integration over \mathbf{q} to be completed. Specializing to the case of constant spin direction $\mathbf{s}_e(\mathbf{r}') = s_e(\mathbf{r}')\hat{\mathbf{s}}$ we get a scattering amplitude

$$f(\mathbf{Q}) = -\mu_n \frac{2m_n}{\hbar^2} \frac{\mu_0 g_e \mu_B}{4\pi} \hat{\mathbf{Q}} \times \hat{\mathbf{s}} \times \hat{\mathbf{Q}} F_{\text{magn}}(\mathbf{Q}), \quad (43)$$

here we see the *magnetic form factor*

$$F^{\text{magn}}(\mathbf{Q}) = \int d\mathbf{r}' e^{i\mathbf{Q}\mathbf{r}'} s_e(\mathbf{r}'). \quad (44)$$

Using the usual cross-product identity $\mathbf{a} \times (\mathbf{b} \times \mathbf{c}) = (\mathbf{a} \cdot \mathbf{c})\mathbf{b} - (\mathbf{a} \cdot \mathbf{b})\mathbf{c}$ one gets $\hat{\mathbf{Q}} \times \hat{\mathbf{s}} \times \hat{\mathbf{Q}} = \hat{\mathbf{s}} - (\hat{\mathbf{s}} \cdot \hat{\mathbf{Q}})\hat{\mathbf{Q}}$; note that this is the component of $\hat{\mathbf{s}}$ perpendicular to $\hat{\mathbf{Q}}$. Thus the scattering amplitude (44) is related to the Fourier transform of the spin density component perpendicular to the scattering vector \mathbf{Q} . So, magnetic neutron scattering allows a determination of both the size and the direction of the magnetisation in a material of interest. Originally neutron scattering was the only practical probe for the determination of the magnetic structure of solids. In the present time magnetic X-ray scattering with X-rays produced using synchrotron radiation sources can also deliver such information.

Let us estimate the magnitude of the magnetic scattering length (43). The neutron magnetic moment is $\boldsymbol{\mu}_n = \frac{1}{2}g_n\mu_N\boldsymbol{\sigma}$, where g_n is the neutron g -factor, μ_N the nuclear magneton and $\boldsymbol{\sigma} = 2\mathbf{s}_n$ is the Pauli spin operator. We can estimate the prefactor in (43) to be

$$\frac{2m_n}{\hbar^2} \frac{\mu_0}{4\pi} g_n \frac{e\hbar}{2m_p} g_e \frac{e\hbar}{2m_e} \approx 4 \frac{e^4}{(4\pi\epsilon_0\hbar c)^2} \frac{4\pi\epsilon_0\hbar^2}{m_e e^2} = 4\alpha^2 a_0,$$

where $g_n \approx -4$, $g_e \approx -2$, $m_n \approx m_p$, $\mu_0 = 1/\epsilon_0 c^2$, the Bohr magneton $\mu_B = e\hbar/2m_e$, the nuclear magneton $\mu_N = e\hbar/2m_p$, the fine structure constant $\alpha = e^2/4\pi\epsilon_0\hbar c$ and the Bohr radius $a_0 = 4\pi\epsilon_0\hbar^2/m_e e^2$ have been used. Note that $\alpha^2 a_0$ is the classical electron radius r_e ; this happens to be in the same range as nuclear scattering lengths b . Thus the nuclear and magnetic scattering are of competitive size (very much unlike the X-ray case); this means that interference between the two forms of scattering can in practice occur.

References

- [1] Wikipedia article, “Klein-Nishina Formula”.
- [2] Wikipedia article, “Atomic Form Factor”.
- [3] Wikipedia article, “X-ray Absorption Spectroscopy”.
- [4] Piero Pianetta, *X-ray data booklet*, http://xdb.lbl.gov/Section3/Sec_3-2.pdf.
- [5] Varley Sears, *Neutron Cross Sections*, Neutron News **3** (3), 26 (1992).